SAND2018-3971C

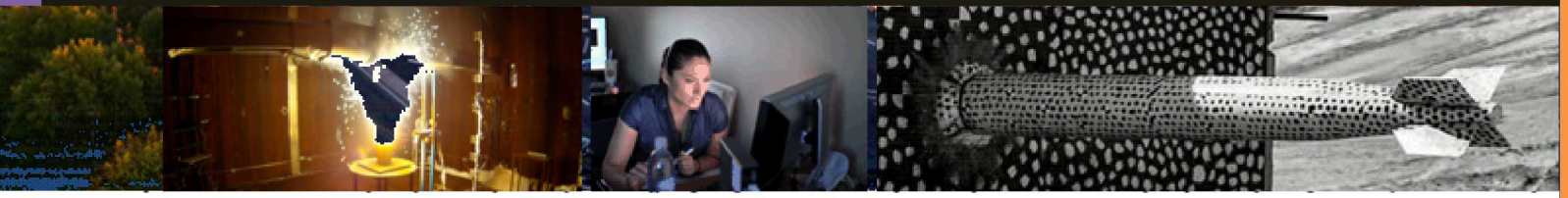

Coupled Magnetic Spin Dynamics and Molecular Dynamics in a Massively Parallel Framework

PRESENTED BY

J. Tranchida, P. Thibaudeau, S. J. Plimpton, A. P. Thompson

Contact: jtranch@sandia.gov

Sandia National Laboratories is a multimission laboratory managed and operated by National Technology and Engineering Solutions of Sandia LLC, a wholly owned subsidiary of Honeywell International Inc. for the U.S. Department of Energy's National Nuclear Security Administration under contract DE-NA0003525.

Outline

- I Introduction
  - Motivations for this development.
  - Basic idea of the methodology.
  - First successes, limitations.
- II Implementation
  - Symplectic SD-MD serial algorithm.
  - Accounting for the temperature effects.
  - Spin-lattice relaxation results.
  - Parallel implementation, accuracy and scalability.
- III Finally doing some physics
  - Implemented magnetic interactions.
  - Parametrization of an interaction (exchange).
  - Example 1: BFO.
  - Example 2: Magnetoelasticity of hcp cobalt.

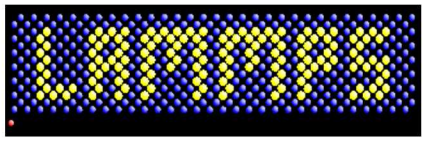

http://lammps.sandia.gov/

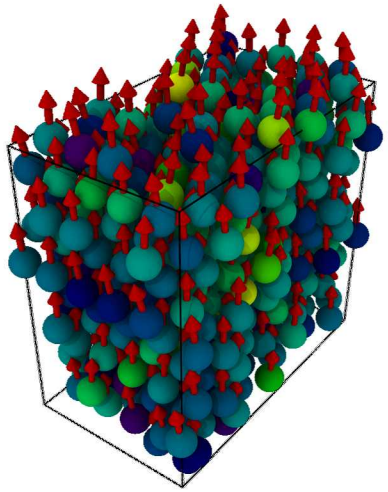

A computational model coupling micro-structure and magnetic properties

Fabrication process

Learning cycles

Micro-structure

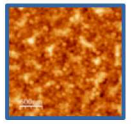

- Defects
- Inhomogeneity
- Composition
- Phase-change (inter-metallic)

Properties

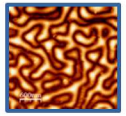

- Magneto-elasticity
- Spin-lattice relaxation
- Magnetization dynamics
- Spin textures

Applications

- Energy (magneto-calorics devices, efficient data storage),
- Multiferroic materials,
- Tagging applications.

Development of a model enhancing those learning cycles, and enabling the study of magnetoelastic effects and of the influence of the micro-structure on the magnetic properties.

Molecular dynamics (MD)

- Enables: defects, inhomogeneity, phase-change
- ✖ Limitations: do not account for magnetization

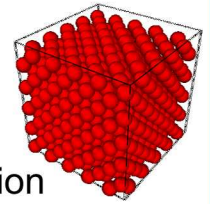

Spin dynamics (SD)

- Enables: magnetization dynamics, spin textures
- ✖ Limitations: structural defects, fixed lattice

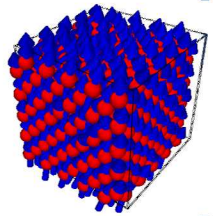

Coupled SD - MD

- Coupled lattice and magnetic spins
- Enables: magneto-elasticity, s-l relaxation, coupled s-l phenomena

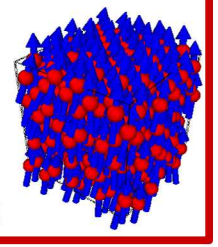

Pictures from MFM measurements performed by T-M Lu, org. 1867

Methodology, first successes, and some current limitations

Methodology

:

Molecular dynamics (MD)

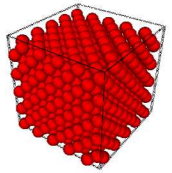

$$\left.\begin{aligned} \frac{\partial \boldsymbol{r}_\mathrm{i}}{\partial t} &= \boldsymbol{v}_\mathrm{i} \\ \frac{\partial \boldsymbol{v}_\mathrm{i}}{\partial t} &= \boldsymbol{F}_\mathrm{i}\left(\boldsymbol{r}_\mathrm{ij}, \boldsymbol{s}_\mathrm{i,j}\right) \end{aligned}\right\}$$

$$\mathcal{H} = \underbrace{\sum_{i=1}^{N} \frac{|\boldsymbol{p}_i|^2}{2m_i} + \sum_{i,j=1}^{N} V\left(r_{ij}\right)}_{\text{MD Hamiltonian}}$$

Coupled SD - MD

$$\left\{\begin{aligned} \frac{\partial \boldsymbol{r}_\mathrm{i}}{\partial t} &= \boldsymbol{v}_\mathrm{i} \\ \frac{\partial \boldsymbol{v}_\mathrm{i}}{\partial t} &= \boldsymbol{F}_\mathrm{i}\left(\boldsymbol{r}_\mathrm{ij}, \boldsymbol{s}_\mathrm{i,j}\right) \\ \frac{\partial \boldsymbol{s}_\mathrm{i}}{\partial t} &= \boldsymbol{\omega}_\mathrm{i} \times \boldsymbol{s}_\mathrm{i} \end{aligned}\right.$$

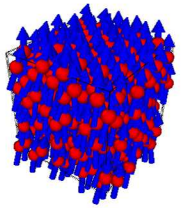

$$\boldsymbol{H}_{sl} = \underbrace{\sum_{i=1}^{N} \frac{|\boldsymbol{p}_i|^2}{2m_i} + \sum_{i,j=1}^{N} V\left(r_{ij}\right)}_{\text{MD Hamiltonian}} \underbrace{- \sum_{i,j,i\neq j}^{N} J\left(r_{ij}\right)\, \boldsymbol{s}_i \cdot \boldsymbol{s}_j - \mu_B \mu_0 \sum_{i=0}^{N} g_i \boldsymbol{s}_i \cdot \boldsymbol{H}_{ext}}_{\text{Spin–lattice coupling}}$$

First successes:

- Simulation of magneto-caloric effects
  - Ma, P. W., & Dudarev, S. L. (2014). Dynamic magnetocaloric effect in bcc iron and hcp gadolinium. Physical Review B, 90(2), 024425.
- Influence of defects on the magnetism of bcc iron
  - Mudrick, M., et al. Combined molecular and spin dynamics simulation of bcc iron with lattice vacancies. In Journal of Physics: Conference Series (Vol. 921, No. 1, p. 012007).
  - Wen, H., Ma, P. W., & Woo, C. H. (2013). Spin-lattice dynamics study of vacancy formation and migration in ferromagnetic BCC iron. Journal of Nuclear Materials, 440(1-3), 428-434.

Some current limitations:

- ✖ No release in an open-source MD code
  - preventing from the development of a large user base
- ✖ Insufficient level of parallelization
  - does not allow the simulation of large magnetic devices
- ✖ Simulation of the spin-orbit coupling
  - many technological application rely on magnetoelasticity
- ✖ Simulation of the long-range dipolar interaction
  - Unable to stabilize the domain structure of actual magnets

- Summary of the introduction:
  - Necessity to develop models coupling micro-structure and magnetic properties.
  - Four limitations of the former implementations were analyzed.

- Next section: Implementation of coupled SD-MD (CS part)
  - Implementation symplectic algorithm for coupled SD-MD.
  - Parallelization, and properties (scalability and accuracy)

Symplectic implementation of SD-MD

Symplectic spin-lattice integration scheme:

- Suzuki-Trotter decomposition applied to the global integration, and to the spin:

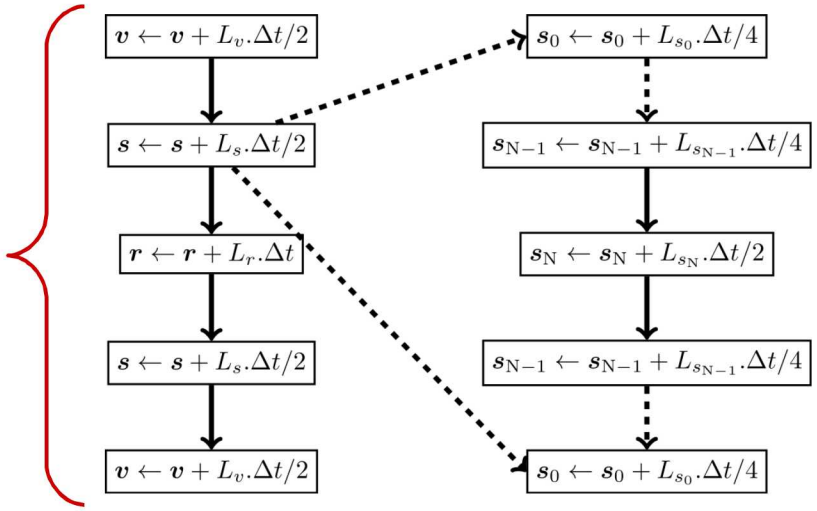

- With Lv, Ls and Lr being the advance operators of the velocities, spins and positions.
- Each spin advance is performed according to a geometric expression accurate in Dt^3.

Accuracy of the numerical scheme:

- Varying the value of the timestep Dt from 0.1 fs to 0.2 ps.

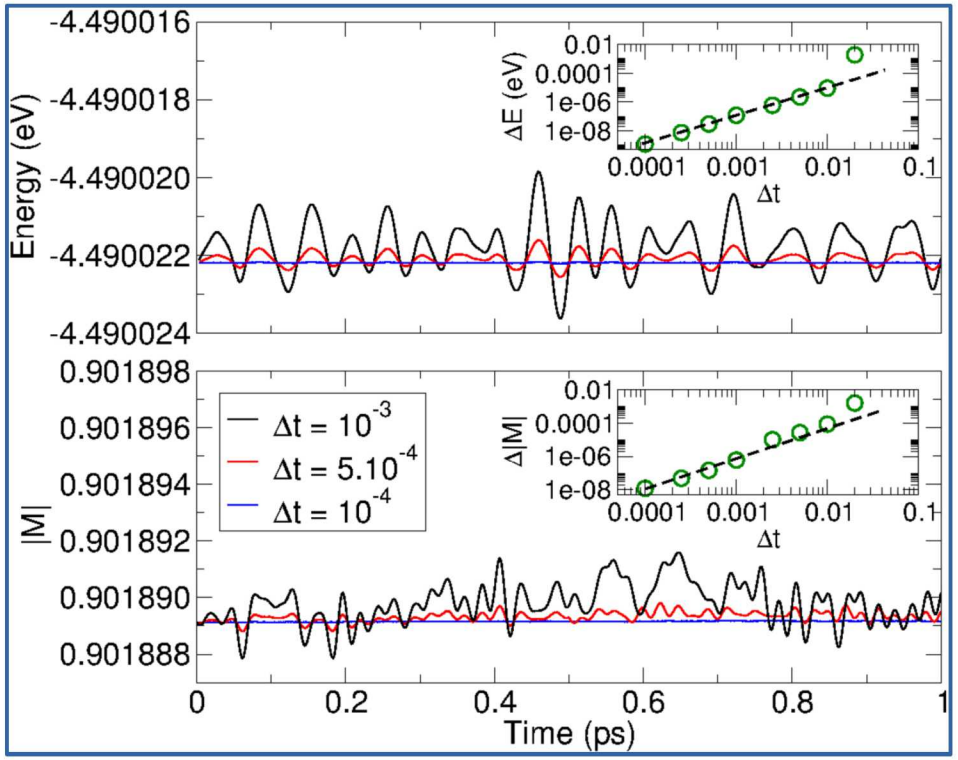

- Numerical accuracy Dt^2 (as expected).

Tranchida, J., Plimpton, S. J., Thibaudeau, P., & Thompson, A. P. (2018). Massively parallel symplectic algorithm for coupled magnetic spin dynamics and molecular dynamics. arXiv preprint arXiv:1801.10233, submitted to Journal of Computional Physics.

Accounting for the temperature effects

Stochastic equations for the spin-lattice system

- Two Langevin thermostats are applied to the lattice and spins systems:

$$\begin{aligned}
\frac{d\boldsymbol{r}_i}{dt} &= \frac{\boldsymbol{p}_i}{m_i} \\
\frac{d\boldsymbol{p}_i}{dt} &= \sum_{j,i\neq j}^{N}\left[-\frac{dV\left(r_{ij}\right)}{dr_{ij}}+\frac{dJ\left(r_{ij}\right)}{dr_{ij}}\boldsymbol{s}_i\cdot\boldsymbol{s}_j\right]\boldsymbol{e}_{ij}-\frac{\gamma_L}{m_i}\boldsymbol{p}_i+\boldsymbol{f}(t) \\
\frac{d\boldsymbol{s}_i}{dt} &= \frac{1}{(1+\lambda^2)}\Big(\left(\boldsymbol{\omega}_i+\boldsymbol{\eta}(t)\right)\times\boldsymbol{s}_i+\lambda\,\boldsymbol{s}_i\times\left(\boldsymbol{\omega}_i\times\boldsymbol{s}_i\right)\Big)
\end{aligned}$$

- The magnetic random torque is defined as a white-noise drawn from a Gaussian distribution:

$$\begin{aligned}
\langle\boldsymbol{\eta}(t)\rangle &= \mathbf{0} \\
\langle\eta_\alpha(t)\eta_\beta(t')\rangle &= 2D_S\delta_{\alpha\beta}\delta(t-t') \\
\text{with } D_S &= \frac{2\pi\lambda k_B T}{\hbar}
\end{aligned}$$

Spin and lattice temperatures

- Spin and lattice temperatures are defined as follow:

$$\begin{aligned}
T_L &= \frac{2}{3\,N\,k_B}\sum_{i=1}^{N}\frac{|\boldsymbol{p}_i|^2}{2m_i} \\
T_S &= \frac{\hbar}{2k_B}\frac{\sum_{i=1}^{N}|\boldsymbol{s}_i\times\boldsymbol{\omega_i}|^2}{\sum_{i=1}^{N}\boldsymbol{s}_i\cdot\boldsymbol{\omega}_i}
\end{aligned}$$

- This spin temperature Ts is a measure of the magnetic disorder in the system:

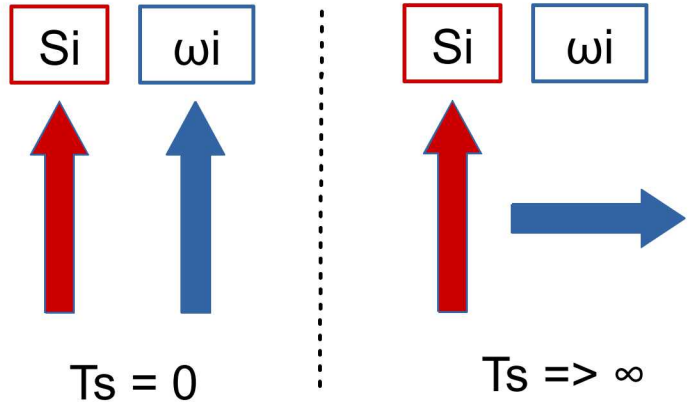

Tranchida, J., Plimpton, S. J., Thibaudeau, P., & Thompson, A. P. (2018). Massively parallel symplectic algorithm for coupled magnetic spin dynamics and molecular dynamics. arXiv preprint arXiv:1801.10233, submitted to Journal of Computional Physics.

Symplectic implementation of SD-MD

Spin-lattice relaxation, NVE calculation

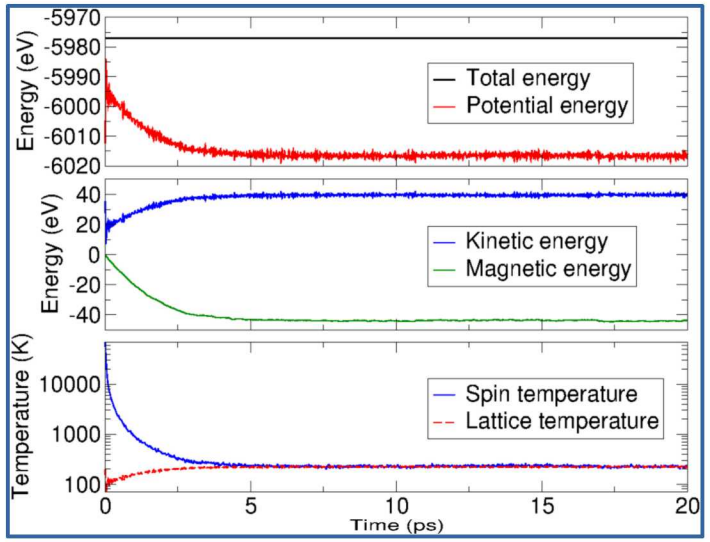

- Parameters of fcc-cobalt.
- Preservation of the total energy as the kinetic, potential and magnetic energy are compensating each others.
- Relaxation and equilibration of the spin and lattice temperatures

Spin-lattice relaxation, NVT calculation

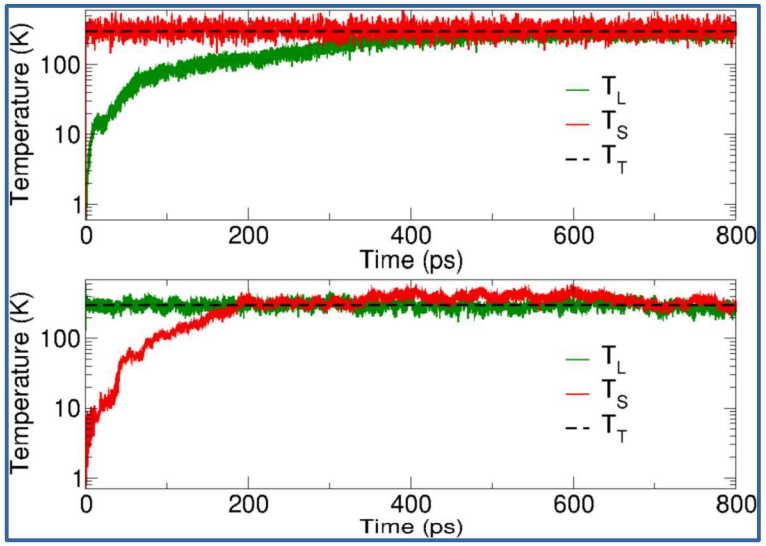

- Parameters of fcc-cobalt
- Langevin thermostat applied to the spins and to the lattice
- Relaxation and equilibration of the spin and lattice temperatures.

Tranchida, J., Plimpton, S. J., Thibaudeau, P., & Thompson, A. P. (2018). Massively parallel symplectic algorithm for coupled magnetic spin dynamics and molecular dynamics. arXiv preprint arXiv:1801.10233, submitted to Journal of Computional Physics.

Sectoring algorithm for scalable SD-MD

- A symplectic sectoring algorithm for massively parallel SD-MD simulations.

Sectoring algorithm for a 2D sample

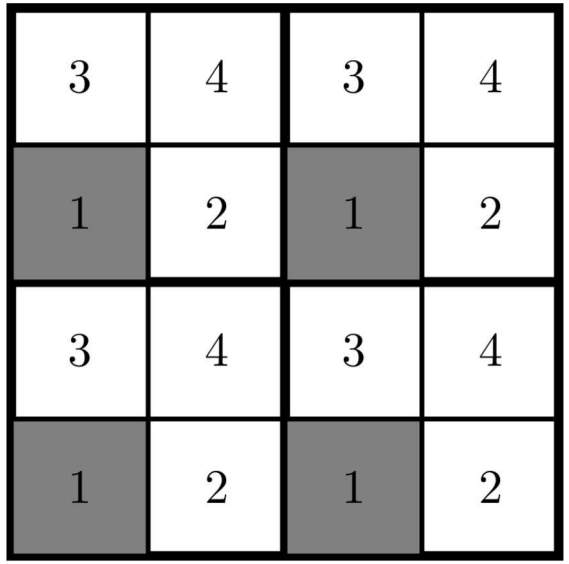

- LAMMPS divide the simulation cell into domains.
- Each domain is divided into sectors (4 in 2D, 8 in 3D).
- Spins in sectors with the same label are sure not to be neighbors: they can be updated simultaneously.

Communication operations between sectors

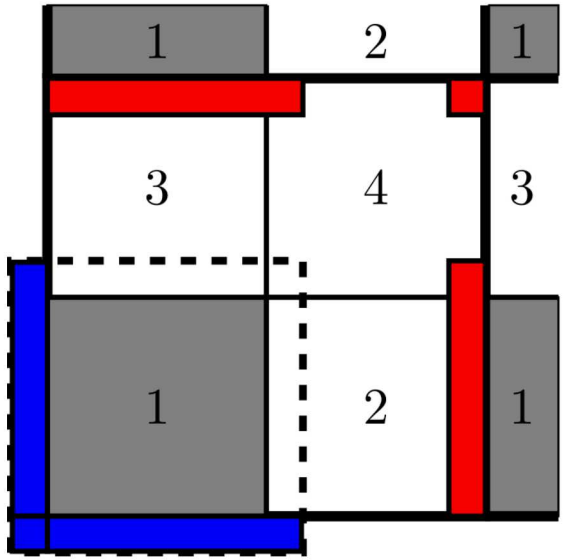

- Focus on the bottom left domain of the previous figure.
- Communication operation after the advance operation of the spins in a sectors labeled 1.
- Red areas have to be sent, the blue ones have to be received from other domains.

Tranchida, J., Plimpton, S. J., Thibaudeau, P., & Thompson, A. P. (2018). Massively parallel symplectic algorithm for coupled magnetic spin dynamics and molecular dynamics. arXiv preprint arXiv:1801.10233, submitted to Journal of Computional Physics.

A scalable implementation of SD-MD in LAMMPS

Accuracy of the parallel algorithm

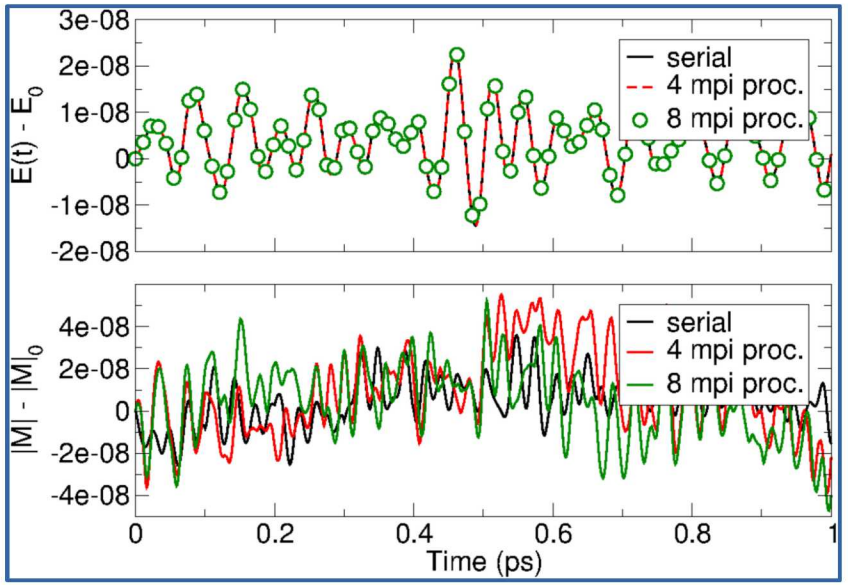

- Error for the total energy and the norm of the magnetization preservation.
- Different trajectories, but nor accuracy loss with the number of precesses.

Parallel efficiency: weak scaling

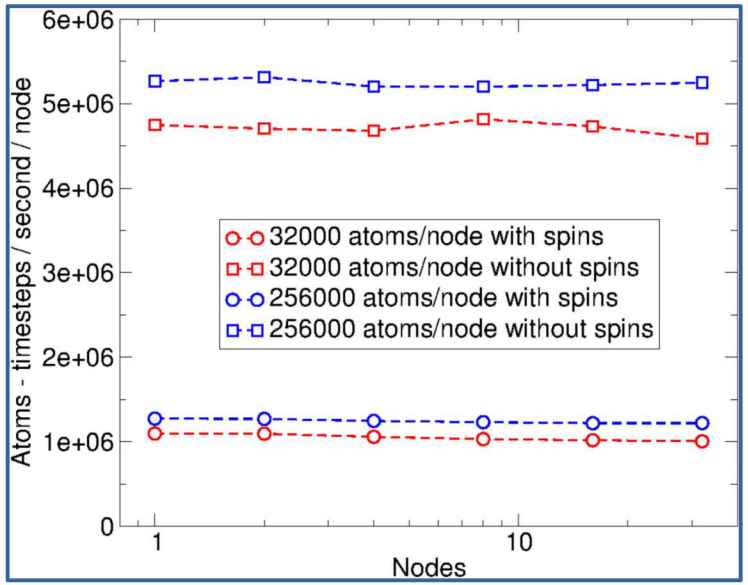

- From 1 to 32 Broadwell nodes, with 36 processes per node (1024 processes for the last point).
- Spin-lattice calculations only 5 times slower than an EAM calculation.

Tranchida, J., Plimpton, S. J., Thibaudeau, P., & Thompson, A. P. (2018). Massively parallel symplectic algorithm for coupled magnetic spin dynamics and molecular dynamics. arXiv preprint arXiv:1801.10233, submitted to Journal of Computional Physics.

- Summary of the CS section:
  - A symplectic scalable algorithm was implemented into LAMMPS
  - This implementation tackles the two first limitations.

- Next section: Implemented physics, and examples
  - Current interactions, and how to parametrize the exchange.
  - Two ongoing examples of applications.

Accounting for the spin-lattice interactions

- The current version accounts for six magnetic interactions:

Exchange interaction:

$$\boldsymbol{H}_{exchange} = -\sum_{i,j,i\neq j}^{N} J\left(r_{ij}\right)\, \vec{s}_i \cdot \vec{s}_j$$

- Simulation of ferromagnetism, antiferromagnetism, ferrimagnetism, ...

Uniaxial anisotropy:

$$\boldsymbol{H}_{an} = -\sum_{i=1}^{N} K_{an}(\boldsymbol{r}_i)\, \left(\boldsymbol{s}_i \cdot \boldsymbol{n}_i\right)^2$$

- Simulation of magnetocrystalline anisotry or shape anisotropy.
- ✖ Poor lattice dependence.

Dzyaloshinskii-Moriya:

$$\boldsymbol{H}_{dm} = \sum_{i,j=1,i\neq j}^{N} \vec{D}\left(r_{ij}\right) \cdot \left(\vec{s}_i \times \vec{s}_j\right),$$

- Simulation of an effect of the spin-orbit coupling
- Very trendy (chiral magnetism, skyrmions...)

Zeeman interaction:

$$\boldsymbol{H}_{Zeeman} = -\mu_B \mu_0 \sum_{i=0}^{N} g_i\, \boldsymbol{s}_i \cdot \boldsymbol{H}_{ext}$$

- Interaction with an external magnetic field (constant or time dependent).

Magneto-electric interaction:

$$\boldsymbol{H}_{me} = -\sum_{i,j,i\neq j}^{N} \left(\vec{E} \times \vec{e}_{ij}\right) \cdot \left(\vec{s}_i \times \vec{s}_j\right),$$

- Interaction between spins and electric dipoles.
- Simulation of multiferroic materials.

Néel pair anisotropy:

$$\boldsymbol{H}_{Néel} = -\sum_{i,j=1,i\neq j}^{N} g_1(r_{ij}) \left((\boldsymbol{e}_{ij} \cdot \boldsymbol{s}_i)(\boldsymbol{e}_{ij} \cdot \boldsymbol{s}_j) - \frac{\boldsymbol{s}_i \cdot \boldsymbol{s}_j}{3} \right)$$

- Other way to account for effects of the spin-orbit coupling.
- Simulation of magnetocrystalline anisotropy and magneto-elasticity.

Parametrization of the exchange interaction

Derivation of a force and a magnetic torque from the Hamiltonian:

$$\boldsymbol{H}_{exchange} = -\sum_{i,j,i\neq j}^{N} J\left(r_{ij}\right)\,\vec{s}_i\cdot\vec{s}_j$$

- Application of the following Poisson bracket:

$$\{f,g\}=\sum_{i=1}^{N}\left[\frac{\partial f}{\partial \boldsymbol{r}_i}\cdot\frac{\partial g}{\partial \boldsymbol{p}_i}-\frac{\partial f}{\partial \boldsymbol{p}_i}\cdot\frac{\partial g}{\partial \boldsymbol{r}_i}-\frac{\boldsymbol{s}_i}{\hbar}\cdot\left(\frac{\partial f}{\partial \boldsymbol{s}_i}\times\frac{\partial g}{\partial \boldsymbol{s}_i}\right)\right]$$

$$\vec{F}_i=\sum_{j}^{Neighbor}\frac{\partial J\left(r_{ij}\right)}{\partial r_{ij}}\left(\vec{s}_i\cdot\vec{s}_j\right)\vec{r}_{ij}$$

- Force applied to the atoms.

$$\vec{\omega}_i=\frac{1}{\hbar}\sum_{j}^{Neighbor}J\left(r_{ij}\right)\,\vec{s}_j$$

- Torque applied to the spins.

Intensity of the coupling:

- Values of the exchange interaction from DFT calculations, or measurement:

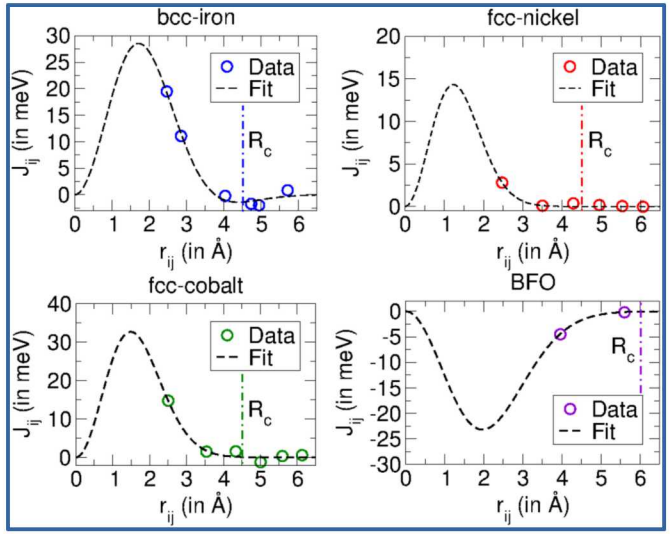

- Function used to fit the discrete values DFT results:

$$J\left(r_{ij}\right)=4a\left(\frac{r_{ij}}{d}\right)^2\left(1-b\left(\frac{r_{ij}}{d}\right)^2\right)e^{-\left(\frac{r_{ij}}{d}\right)^2}\Theta(R_c-r_{ij})$$

Yang, K. H., et al. (1980). Generalizations of classical Poisson brackets to include spin. Phys. Rev. A, 22(5), 1814.

Example 1: multiferroicity and spin textures in bismuth oxide $BiFeO_3$ (BFO)

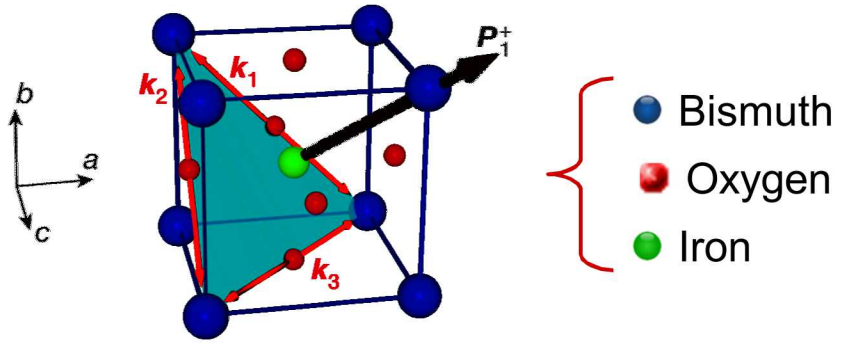

- Bismuth
- Oxygen
- Iron

- A 64 nm long cycloid appears due to the interplay between magnetic and ferroelectric orders:

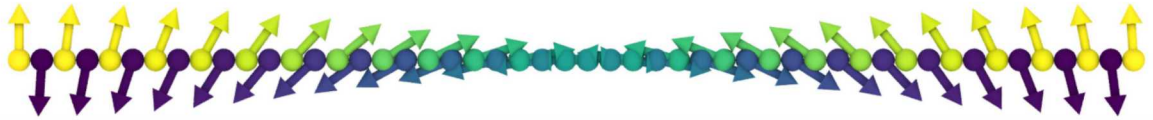

BFO Hamiltonian:

- We first only account for the iron atoms.
- The simulations are performed on a fixed lattice, using the following Hamiltonian:

$$\mathcal{H}_{\mathrm{BFO}} = \underbrace{-\sum_{i,j,i\neq j}^{N} J\left(r_{ij}\right)\, \boldsymbol{s}_i \cdot \boldsymbol{s}_j}_{\text{AF exchange interaction}} + \underbrace{\sum_{i,j=1,i\neq j}^{N} \left(\boldsymbol{E} \times \boldsymbol{e}_{ij}\right) \cdot \left(\boldsymbol{s}_i \times \boldsymbol{s}_j\right)}_{\text{ME interaction}} \underbrace{-\sum_{i=1}^{N} K_{an}(\boldsymbol{r}_i)\, \left(\boldsymbol{s}_i \cdot \boldsymbol{n}_i\right)^2}_{\text{Anisotropy}}$$

Parameters:

- AF exchange interaction:
  - J_1 = -4.38 meV
  - J_2 = - 0.2 meV
- Magneto-electric interaction:
  E = 0.109 meV along [111]
- Magnetic anisotropy:
  K_{an} = 0.0033meV along [111]

Fishman, R. S., et al. (2013). Terahertz Spectroscopy of Spin Waves in Multiferroic BiFeO 3 in High Magnetic Fields. Phys. Rev. Lett., 110(25), 257201.

Example 1: multiferroicity and spin textures in bismuth oxide $BiFeO_3$ (BFO)

- Experimental target:

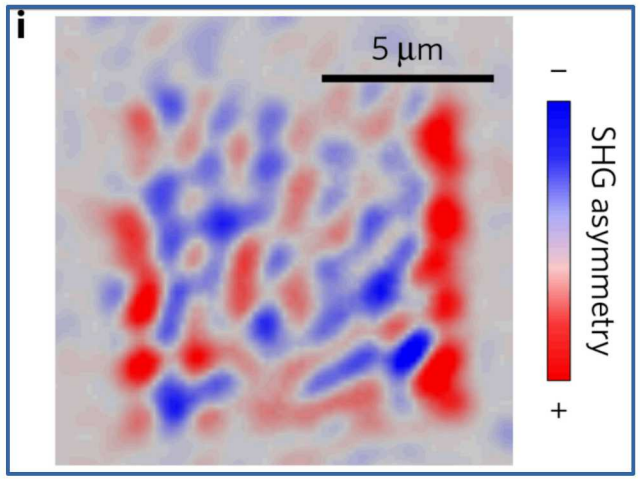

- First numerical results:
  - Equilibrium configuration after relaxation:

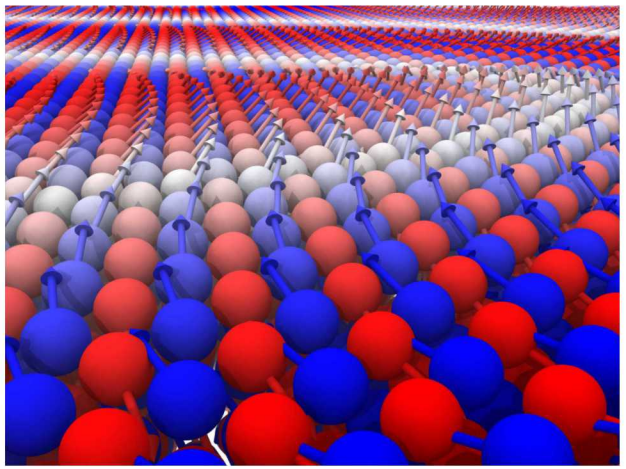

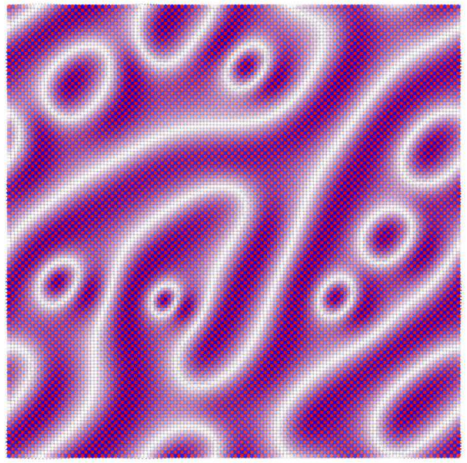

Chauleau, J. Y., Viret, M et al. (2017). Multi-stimuli manipulation of antiferromagnetic domains assessed by second-harmonic imaging. Nature materials, 16(8), 803.

- Perspectives:
  - Phase diagram of the existence of the antiferromagnetic bubbles.
  - Find the correct interactions to perform full magneto-electric and elastic simulations.

Juraschek, D. M., et al. (2017). Dynamical multiferroicity. Phys. Rev. Mat., 1(1), 014401.

Example 2: magnetoelasticity of hcp cobalt

- Exchange interaction and EAM potential;

$$\mathcal{H}_{\mathrm{hcp-Co}} = \sum_{i=1}^{N} \frac{|\boldsymbol{p}_i|^2}{2m_i} + \underbrace{\sum_{i,j=1}^{N} V(r_{ij})}_{\text{EAM potential} \Rightarrow (1)} - \underbrace{\sum_{i,j,i\neq j}^{N} J(r_{ij})\, \boldsymbol{s}_i \cdot \boldsymbol{s}_j}_{\text{Exchange interaction} \Rightarrow (2)}$$

1 Pun, G. P. et al.. (2012). Phys. Rev. B, 86(13), 134116.

2 Sabiryanov, R. F. et al.. (1999). Phys. Rev. Lett., 83(10), 2062.

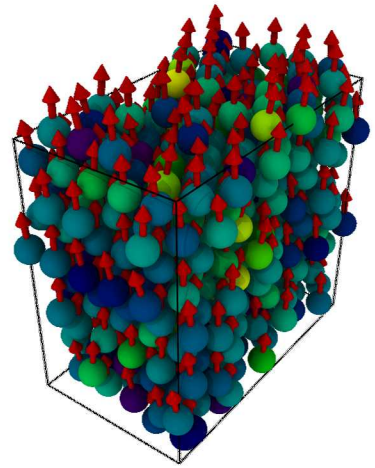

- Spin-orbit coupling and magneto-elastic effects with Néel dipolar and quadrupolar functions:

$$\mathcal{H}_{N\acute{e}el} = -\sum_{i,j=1,i\neq j}^{N} g_1(r_{ij})\left((\boldsymbol{e}_{ij}\cdot\boldsymbol{s}_i)(\boldsymbol{e}_{ij}\cdot\boldsymbol{s}_j) - \frac{\boldsymbol{s}_i\cdot\boldsymbol{s}_j}{3}\right) + q_1(r_{ij})\left((\boldsymbol{e}_{ij}\cdot\boldsymbol{s}_i)^2 - \frac{\boldsymbol{s}_i\cdot\boldsymbol{s}_j}{3}\right)\left((\boldsymbol{e}_{ij}\cdot\boldsymbol{s}_i)^2 - \frac{\boldsymbol{s}_i\cdot\boldsymbol{s}_j}{3}\right) + q_2(r_{ij})\Big((\boldsymbol{e}_{ij}\cdot\boldsymbol{s}_i)(\boldsymbol{e}_{ij}\cdot\boldsymbol{s}_j)^3 + (\boldsymbol{e}_{ij}\cdot\boldsymbol{s}_j)(\boldsymbol{e}_{ij}\cdot\boldsymbol{s}_i)^3\Big)$$

Pair model from the magnetostriction constants

- Following Cullen's approach, magnetostriction constants can be expressed as functions of g1, q1, and q2.
- Knowing the experimental values of λ , one can fit the constant g1, q1 and q2.
- Using spin-dependent DFT to check the obtained energy surface.

$$\begin{aligned}
\lambda_1^{\alpha} &= \frac{-B_1^{\alpha}\left[g_1(r_{ij}), q_1(r_{ij}), q_2(r_{ij})\right]}{C_1^{\alpha}} \\
\lambda_2^{\alpha} &= \frac{-B_2^{\alpha}\left[g_1(r_{ij}), q_1(r_{ij}), q_2(r_{ij})\right]}{C_2^{\alpha}} \\
\lambda^{\epsilon} &= \frac{-B^{\epsilon}\left[g_1(r_{ij}), q_1(r_{ij}), q_2(r_{ij})\right]}{C_{44}} \\
\lambda^{\gamma} &= \frac{-B^{\gamma}\left[g_1(r_{ij}), q_1(r_{ij}), q_2(r_{ij})\right]}{C_{11}-C_{22}}
\end{aligned}$$

Target result

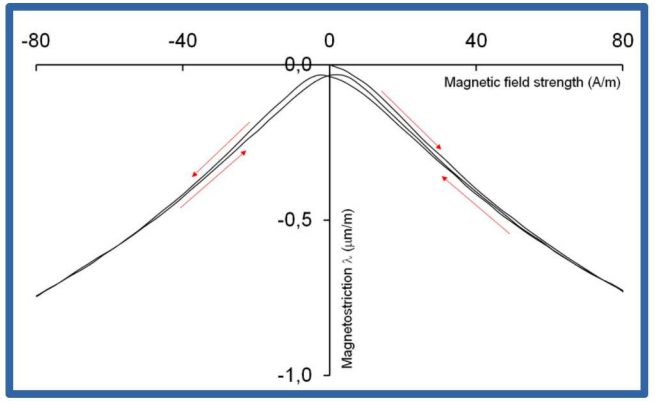

*Cullen, J. R. (1995). Pair model of magnetostriction for hexagonal close-packed crystals. Phys. Rev. B, 52(1), 57.

Summary of the physics section:

- The current implementation accounts for six interactions.
- The exchange interaction can be parametrized as a function of the interatomic distance.
- The simulation of BFO opens the door to coupled magneto-electric and elastic simulations.
- We started to work on the development of models accounting for the effects of the spin-orbit coupling.

Perspectives, future work

Models of spin-orbit coupling

- Current model: pair Néel anisotropy, fitted for hcp cobalt:

$$\mathcal{H}_{\mathrm{N}} = \sum_{\mathrm{i,j,i\neq j}}^{N} g_1(r_{\mathrm{ij}}) \left((\boldsymbol{e}_{\mathrm{ij}} \cdot \boldsymbol{s}_{\mathrm{i}})(\boldsymbol{e}_{\mathrm{ij}} \cdot \boldsymbol{s}_{\mathrm{j}}) - \frac{1}{3} \boldsymbol{s}_{\mathrm{i}} \cdot \boldsymbol{s}_{\mathrm{j}} \right)$$

- Second approach: using spin-dependent DFT to fit g1, q1 and q2, and check the obtained magnetostriction constants.
- Next steps: test this model and develop new ones for cubic crystals.
- Application to the simulation of magnetostriction if FeCo alloys for resonator devices.

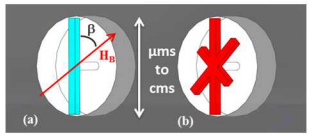

Single- (a) and multi-frequency (b) resonators

Long-range interaction

$$\mathcal{H}_{\mathrm{Mag}} = \underbrace{-\sum_{\mathrm{i,j,i\neq j}}^{\mathrm{N}} \mathrm{J}_{\mathrm{ij}}\,(r_{\mathrm{ij}})\, \boldsymbol{s}_{\mathrm{i}} \cdot \boldsymbol{s}_{\mathrm{j}}}_{\text{exchange interaction}} \underbrace{-\frac{\mu_0 \mu_b^2}{4\pi} \sum_{\mathrm{i,j,i\neq j}}^{\mathrm{N}} \frac{g_{\mathrm{i}} g_{\mathrm{j}}}{r_{\mathrm{ij}}^3} \left((\boldsymbol{s}_{\mathrm{i}} \cdot \boldsymbol{e}_{\mathrm{ij}})(\boldsymbol{s}_{\mathrm{j}} \cdot \boldsymbol{e}_{\mathrm{ij}}) - \frac{1}{3}(\boldsymbol{s}_{\mathrm{i}} \cdot \boldsymbol{s}_{\mathrm{i}}) \right)}_{\text{long-range dipolar interaction}}$$

- A direct calculation of this long-range Hamiltonian would scale as N^2.
- We want to adapt a P3M to magnetic dipoles will be performed (scaling of N.log(N)).
- Application: simulation of the influence of a phase-change on the magnetic domain configuration.

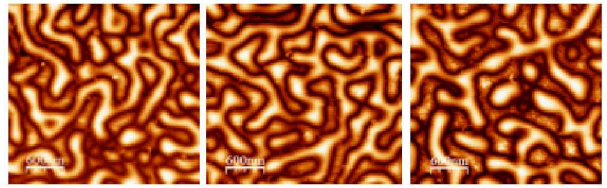

MFM measurements by T-M Lu, Sandia Labs

Conclusions

Conclusions:

- A massively parallel implementation of spin-lattice dynamics was implemented into LAMMPS (open release within the next months).
- The model adds new physics into LAMMPS, is accurate, scales very well with the number of processes, and only 5 times slower than usual MD – EAM calculations.
- Accounts for a lot of magnetic interactions, but models for the spin-orbit coupling and the long-range exchange interaction still need to be developed.
- Open to collaborations, feel free to contact us (jtranch@sandia.gov).

- Thanks to my group at Sandia:
  Aidan Thompson, Steve Plimpton, Mitch Wood, Stan Moore, Veena Tikare.
- And to my Ph.D. advisor in France:
  Pascal Thibaudeau.

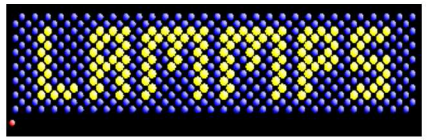

http://lammps.sandia.gov/

Thank you your hosting me and for you attention.